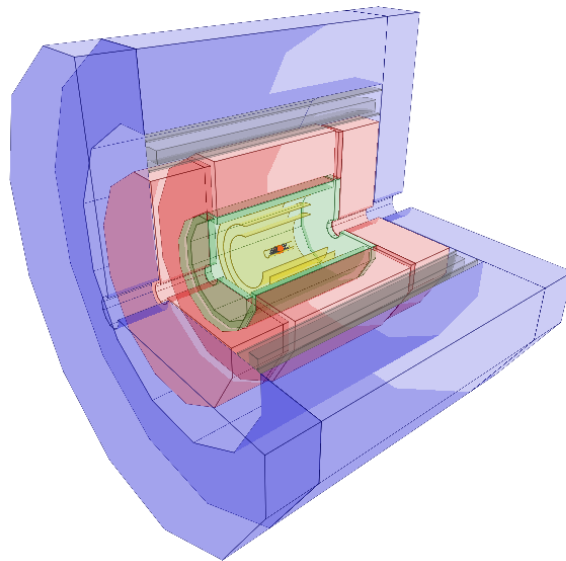


## 1 Detector (D. Lucchesi)

### 1.1 Concepts (L.Sestini, D. Zuliani)

#### 1.1.1 System overview

The detector concept for a  $\sqrt{s} = 3$  TeV muon collider is based on the detector proposed by CLIC [1], with few modifications to adapt it to the machine-detector interface. To accommodate the large physics program expected, an angular coverage close to  $4\pi$  is required. The angular coverage is limited by the presence of the nozzles, two double-cone shielding absorbers made of tungsten and borated polyethylene having an opening angle of  $10^\circ$ , which are necessary to mitigate the impact of the BIB. The nozzles are placed along the beam axis, in the region between 6 and 600 cm away from the interaction point. The innermost system closest to the beam-pipe is a full-silicon tracking system, that includes a vertex detector made of silicon pixels with double layers, and inner and outer trackers respectively composed of silicon macropixels and microstrips. The tracking system is surrounded by a calorimeter system consisting of an electromagnetic (ECAL) and hadronic (HCAL) calorimeter, the former composed of alternating layers of tungsten absorber and silicon sensors, the latter has alternating layers of steel absorber and scintillating pads. A solenoid with an inner bore of 3.5 m radius, provides a magnetic field of 3.57 T, whose flux is returned by a magnet iron yoke which surrounds HCAL, instrumented with muon chambers (resistive plate chambers). A scheme of the full detector is shown in Figure 1.1.



**Fig. 1.1:** Muon collider detector concept. From the innermost to the outermost regions, it includes the tracking system (yellow), the electromagnetic calorimeter (green), the hadronic calorimeter (red), the superconducting solenoid (gray), and muon detectors (blue).

#### 1.1.2 Key challenges

As for the accelerator, the main technological challenges for the detector arise from the short lifetime of muons. In fact the beam-induced background (Section ??), produced by the decay in flight of muons in the beams and subsequent interactions, potentially poses a serious limitation to detector operations. All

kinds of particles are produced, like photons, electrons, and neutrons, that can be partially mitigated by a proper design of the machine-detector-interface, as described in Section ???. Nevertheless, an order of  $10^8$  particles enter the detector, therefore the detector design, the technology choices, and the reconstruction strategies must primarily take into account the beam-induced-background impact.

It is important to study the features of the beam-induced background by using simulation, in order to take the proper directions for the detector development. Figure 1.2 shows two key distributions, the arrival time (normalized to the bunch crossing time) and the energy of the beam-induced background particles when they enter the detector. These distributions have been obtained from the MARS15 simulation at  $\sqrt{s} = 1.5$  TeV (Section ???). It can be seen that most beam-induced background particles are asynchronous with respect to the bunch crossing, and they usually have low energy, therefore timing measurements and appropriate energy thresholds are important handles to suppress them at the detector level.

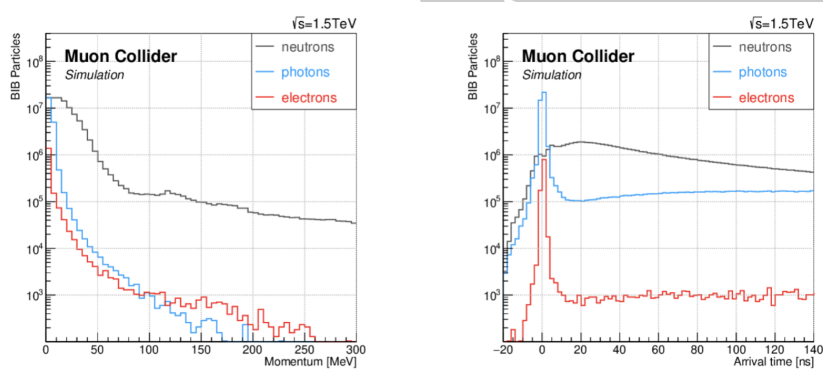


**Fig. 1.2:** Energy and arrival time, normalized to the bunch crossing time, of the beam-induced background particles when they enter the detector.

The following general requirements have been identified for the detector, driven by the necessity of suppressing the beam-induced background and keeping the signal efficiencies as high as possible:

- time measurements with excellent resolution, ranging from 30 to 60 ps for the tracking system, and around 100 ps for the calorimeters;
- energy measurements, to apply the proper threshold for rejecting the beam-induced background soft component;
- high granularity, to reduce the overlaps between beam-induced background and signal hits, and consequently reducing the occupancy;
- radiation hard devices, since the radiation level is similar to what is expected at the High Luminosity LHC (HL-LHC) [2].

The research and development for these technologies have to be performed in synergy with the existing programs, from HL-LHC to other future colliders.

The muon collider detector should ensure the physics reaches from low energy (*e.g.* Higgs and standard model physics) to the highest achievable energy scale for new physics searches (Section ???). This is particularly challenging in the detector for  $\sqrt{s} = 10$  TeV collisions and beyond, where particle momenta from few GeV to several TeV have to be measured. The detector layout and design should cope

with these physics requirements, and at the same time, it has to accommodate the MDI requirements and geometry. In this context, the choice of the magnetic field is of paramount importance. High magnetic fields (4 T and above) could help in improving tracking momentum resolution, but the construction of such magnets is not trivial. In fact, there are significant challenges to achieve the mechanical and electrical stability of this kind of superconductive solenoids, including the technology transfer from previous HEP projects and the availability of experts.

Another challenge, but not the least important, is the simulation of the detector for reconstruction and performance studies. The propagation of millions of beam-induced background particles through the detector volume, performed with software based on Geant4 [3], is heavily time-consuming. Dedicated software and algorithms that tackle this problem in the proper way should be developed since the muon collider environment is different from that of other well-known collider machines. Adequate computing resources should also be allocated for the detector studies.

### 1.1.3 Work progress since Roadmap

An important progress since the last European Strategy for Particle Physics update is the first set of studies for the development of the detector concept at  $\sqrt{s} = 10$  TeV. To properly understand the required specifications, the physics of  $\sqrt{s} = 10$  TeV collisions is considered. We identified two macro-categories of physics processes:

- low energy physics process: typical examples are Electroweak (EW) and Higgs production, with energy in the range of a few hundreds of GeV;
- high energy physics process: New Physics (NP) processes can create heavy resonances ( $Z'$ ) at the order of TeVs;
- unconventional signatures: long-lived particles, disappearing tracks, and emerging jets are just a few examples.

As a reference, the transverse momenta  $p_T$  of the decay products for Higgs production and  $Z'$  production are shown in Figure 1.3.

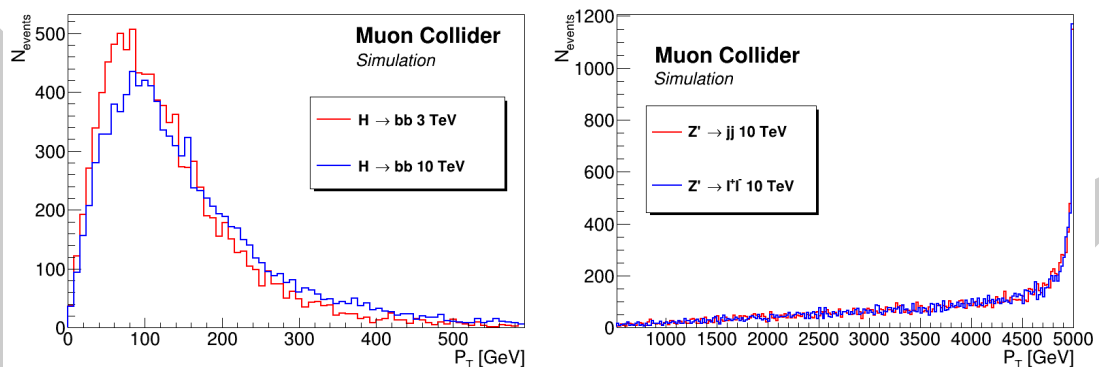


**Fig. 1.3:** Left:  $b$ -quark  $p_T$  distributions from the  $H \rightarrow b\bar{b}$  decays at  $\sqrt{s} = 3$  and 10 TeV, as obtained at generator level. Right: distribution of leptons and jets  $p_T$  from the decay of a  $Z'$  produced at  $\sqrt{s} = 10$  TeV with a mass of 9.5 TeV, as obtained at generator level.

A detector for a 10 TeV muon collider should be able to properly measure these categories of

physics processes. The design of the detector goes through the optimization of the different subdetectors. For the tracking system, a parametric study has been done showing the relation between the depth of the tracking system and the magnetic field. Figure 1.4 (left) shows the results for tracks with a transverse momentum  $p_T \sim 5000$  GeV, where it is evident that a deeper tracker with a higher magnetic field is necessary to keep a good track reconstruction resolution. The choice of the magnetic field is crucial, as well as the layout of the magnet. A preliminary discussion with magnets experts has been done at CERN in a dedicated workshop [?], that set the basis for future studies. For the calorimeter system, studies with photon/protons/pions particle guns have been done, and they have demonstrated the necessity of having deeper calorimeters to contain the shower. As an example, Figure 1.4 (right) shows an evident leakage into HCAL for photons with energies greater than 1 TeV. For the muon reconstruction, studies on muon with  $p_T \sim 5000$  GeV have shown that more inclusive algorithms that use also calorimeters information should be used in order to collect the energy released by muons.

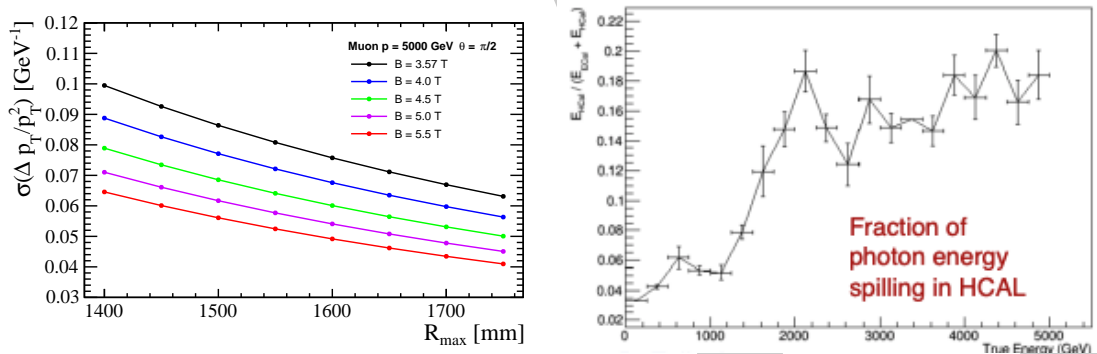


**Fig. 1.4:** Left: track momentum resolution for muons with  $p = 5$  TeV, as a function of the tracker radius ( $R_{max}$ ) and for different values of magnetic field ( $B$ ). Right: fraction of photon energy released in HCAL with respect to the total energy in ECAL+HCAL, as a function of the true photon energy.

#### 1.1.4 Work planned for Evaluation Report

An important step that has to be taken for the Evaluation Report, is the assessment of the  $\sqrt{s} = 10$  TeV beam-induced background effects on the detector. This will include the study of incoherent electron-positron production, which is a feature that arises at very high energy collisions. Once the simulation samples of the  $\sqrt{s} = 10$  TeV beam-induced background described in Section ?? will be validated, the studies at detector level will start. First, the interactions of the beam-induced background with the detector have to be simulated with the muon collider software framework, by using preliminary  $\sqrt{s} = 10$  TeV detector layouts. A few configurations with different magnetic field will be considered. At this point, several important features like the detector occupancies and the distributions of hit position, time, and energy will be studied. A new evaluation of radiation levels will be also performed. The detector requirements will be reviewed, to understand if important changes for the detector layout and technology choices are necessary, with respect to the  $\sqrt{s} = 3$  TeV concept. The reconstruction performance of the fundamental physics objects will be studied, at the beginning with the same algorithms reported in Section ??, and on a second time with algorithms tuned specifically for the  $\sqrt{s} = 10$  TeV case. Feedback to the MDI study group will be given, in order to understand if it will be possible to improve the detector acceptance (*e.g.* reducing the nozzles angle) by keeping at the same time an excellent reconstruction performance.

The studies on the  $\sqrt{s} = 10$  TeV detector will be put together to obtain one of the most important milestones of the project, the definition of the  $\sqrt{s} = 10$  TeV detector concept. The magnet layout and magnetic field intensity will be established, this choice will drive the displacements of the other detector sub-systems. The tracking, calorimeter, and muon detector system geometries will be defined, considering the available space (limited by the magnet, MDI, and cavern dimensions). The target technologies will be assumed, according also to some cost considerations. The  $\sqrt{s} = 10$  TeV detector concept will be implemented in a future release of the muon collider simulation framework and will be the starting point for all future studies. The simulation of the beam-induced background in this detector will be provided, as well as a version of the reconstruction algorithm with an initial tune for this concept.

### ***1.1.5 Important missing effort***

An important aspect that is not yet developed, is the feasibility of a system for the detection of very forward muons. These muons are emitted outside the detector acceptance, but they could be important for physics measurements. As an example muons from  $Z^0 Z^0$  fusion processes are mainly emitted in these regions, therefore their detection could be employed to tag such events. These muon detectors have to be placed along the beam line, where also the accelerator magnets are displaced. The propagation of the very forward muons through these magnetic fields and accelerator components is not trivial, and a dedicated study with Fluka should be performed. The position of the forward muon detectors depends on the available space and from the muon spread in that plane orthogonal to the beam axis. It should be also understood if a rough estimate of the muon momentum could be obtained by measuring the position of the muon hits. All these studies need a dedicated effort that is currently missing in the project.

## **1.2 Performance (M. Casarsa)**

This section presents an overview of the performance of the 3-TeV detector concept for the reconstruction of the primary physics objects in the presence of beam-induced background.

### ***1.2.1 Overview of the physics objects reconstruction***

The high levels of beam-induced background in the detector pose unprecedented challenges for the reconstruction and identification of the particles produced in muon collisions, which are referred to as physics objects. To fully exploit the physics potential of a muon collider and accomplish its physics program, it is essential to reconstruct all the physics objects with high efficiency and determine their properties with the greatest precision, even in the presence of machine-induced background.

A campaign of studies, based on a detailed detector simulation, was carried out to assess the effects of the background on the detector response. The outcome was that the reconstruction algorithms for all the considered physics objects required revision or fine-tuning. However, the results indicate that the background effects on the detector response can be minimized to a degree that does not compromise the detector performance. The detector performance was then estimated reconstructing a set of representative Higgs boson physics channels at a 3 TeV muon collider.

The muon collider software framework [4] is based on CLIC's iLCSoft. It includes the DD4hep toolkit [5] to model the detector geometry, the GEANT4 [3] program to simulate the detector response, and the Marlin package [6] for the event reconstruction.

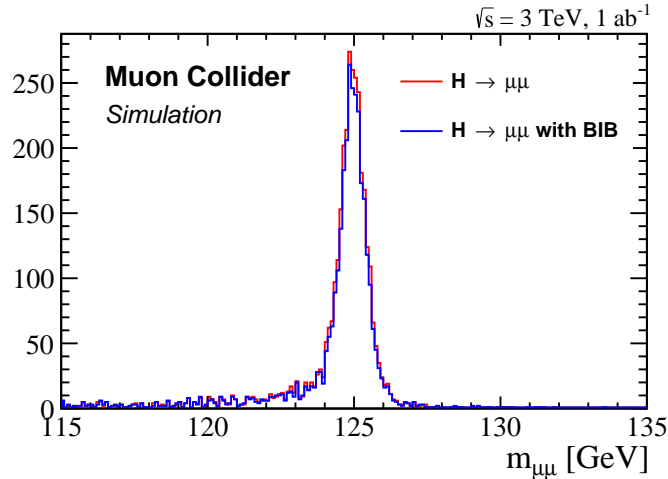


**Fig. 1.5:** Invariant mass distribution of the muon pairs produced in the  $\mu^+\mu^- \rightarrow H\nu_\mu\bar{\nu}_\mu \rightarrow \mu^+\mu^-\nu_\mu\bar{\nu}_\mu$  process without the beam-induced background (red line) and with the beam-induced background overlaid to the physics events (blue line).

The BIB causes very high hit multiplicities in the detector’s tracking system, making the track finding process highly challenging, since the number of hit combinations to be considered increases exponentially, and a uniform diffuse energy deposition in the calorimeters, which makes it difficult to identify and accurately measure the energy of particles from collisions.

In general, the physics objects reconstruction involves combining information from different detector sub-systems. Tracks, calorimeter clusters, and muon detector hits are combined to achieve an optimal performance in terms of identification efficiency, background rejection, and momentum resolution. For this purpose, a particle flow algorithm is employed, PandoraPFA [7], which takes as an input the reconstructed tracks and the hits of the calorimeters and muon detectors.

The initial focus was on muons, electrons, photons, and jets. Muons are identified by matching tracks with hits in the muon detector system. This sub-detector is not significantly affected by the BIB, except for the forward region with respect to the beam direction. Electrons and photons are reconstructed by matching tracks with clusters in the electromagnetic calorimeter. Isolated clusters are classified as photons, while clusters matched with a track are classified as electrons. The energy of electrons and photons is corrected to take into account inefficiencies and radiation losses. The reconstruction efficiency of the electromagnetic objects as a function of the energy reaches around 95% for high energy, but drops at low energies due to the BIB. The particles reconstructed by PandoraPFA are used as input to the jet clustering algorithm, which aims to group together particles produced in the fragmentation process of the same quark or gluon, by exploiting their correlations. The resulting jet energy is corrected to recover the losses due to particles escaping the detector, detector inefficiencies, and also for the BIB contamination. The jet reconstruction algorithm has been tested with simulated samples of different jet flavours: gluons and  $b$ ,  $c$ ,  $u$ ,  $d$ , and  $s$  quarks. Despite the presence of BIB throughout the detector, the efficiency ranges between 80% and 95%, with a negligible fake jet probability. In order to identify the jets originating from heavy quarks, secondary vertices compatible with the decays of  $b$ - and  $c$ -hadrons are reconstructed by combining tracks. A jet is identified as a heavy-flavour jet if one of these secondary vertices is reconstructed within the jet cone. The  $b$ -jet identification probability is of approximately 45% at low



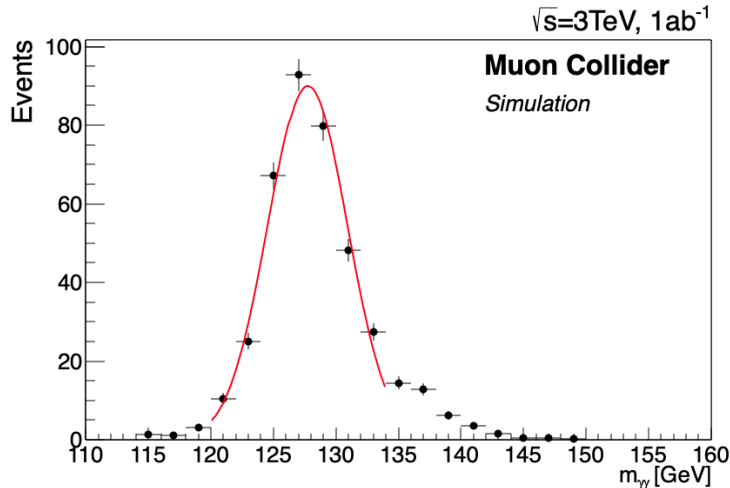


**Fig. 1.6:** Invariant mass distribution of the photon pairs produced in the  $\mu^+\mu^- \rightarrow H\nu_\mu\bar{\nu}_\mu \rightarrow \gamma\gamma\nu_\mu\bar{\nu}_\mu$  process with the beam-induced background overlaid to the physics events.

$p_T$  (20 GeV) and increases to 70% at 120 GeV. This level of performance is similar to what is currently achieved at hadron colliders. At lepton colliders, a higher efficiency is expected. The current algorithm is mainly limited by the presence of the BIB. In the future, artificial-intelligence-based methods will be implemented to minimize the effects of BIB and further enhance efficiency.

The physics objects described above were used to reconstruct the Higgs boson decay modes into the final states  $b\bar{b}$ ,  $\gamma\gamma$ ,  $\mu^+\mu^-$ . The Higgs boson mass distributions give a general indication of the quality of reconstruction for muons, photons, and jets. In fact, the invariant mass depends on the magnitude and the direction of the particle momenta. The peak position at the nominal mass of the Higgs boson indicates a well-calibrated energy of the objects, while the peak width reflects the accuracy with which the object properties are measured. Figures 1.5, 1.6, and 1.7 show the distributions of the Higgs boson reconstructed masses for the process  $\mu^+\mu^- \rightarrow H\nu_\mu\bar{\nu}_\mu$  with  $H$  decaying into  $\mu^+\mu^-$ ,  $\gamma\gamma$ , and  $b\bar{b}$  pairs, respectively. The reconstruction of high-energy muons and photons produced in Higgs boson decays are not significantly affected by the BIB. The dimuon and diphoton peaks exhibit the typical widths for electron-positron colliders: 0.4 GeV and 3.2 GeV, respectively. The case is different for hadronic jets that are also reconstructed with low-energy objects. The reconstruction performance of low-momentum tracks and low-energy calorimeter clusters is impacted by the BIB. The dijet mass resolution is critical, for example to separate the  $H$  and  $Z$  peaks. The current value of the Higgs boson mass resolution is of about 18%, being dominated by BIB effects, *i.e.* the energy thresholds set on the calorimeter hits.

### 1.2.2 Key challenges

The main result of the initial studies with the detailed detector simulation is that the effects of the BIB on high-energy objects in the central region of the detector are negligible. Key challenge in the physics object reconstruction is to reconstruct physics objects with low energy and physics objects in the forward and backward regions of the detector.

The BIB mitigation measures must be refined and perfected in order to improve the reconstruction of the low-energy objects. For instance, the energy thresholds on the calorimeter hits affect the energy resolution of jets and low-energy photons and electrons. In the detector forward and backward regions

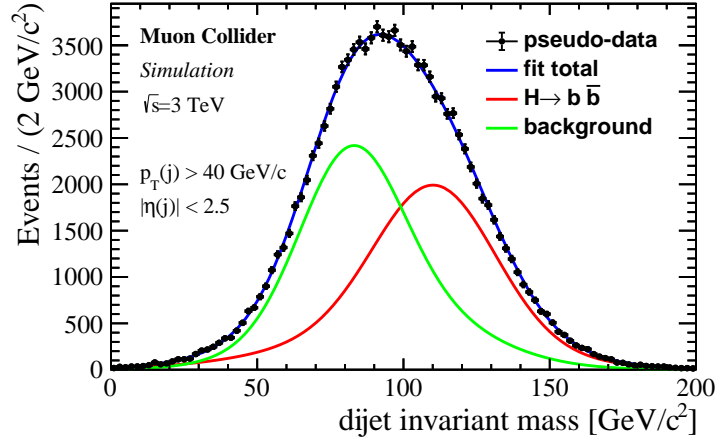


**Fig. 1.7:** Invariant mass distribution of the jet pairs produced in the  $\mu^+\mu^- \rightarrow H\nu_\mu\bar{\nu}_\mu \rightarrow b\bar{b}\nu_\mu\bar{\nu}_\mu$  process with the beam-induced background overlaid to the physics events: the reconstructed mass peak of the Higgs boson is indicated in red, while the background from  $Z \rightarrow b\bar{b}$  and  $Z \rightarrow c\bar{c}$  is in green.

closer to the beamline, the BIB levels are higher. At multi-TeV collision energies, all the standard model particles are highly boosted in the forward region and their decays may produce particles that are very close to each other in space or even overlapping in the detector. Dedicated algorithms must be developed for those cases.

### 1.2.3 Work progress since Roadmap

Since the Roadmap, an assessment has been performed of the reconstruction performance for tracks, muons, electrons, photons, and jets in the presence of the beam-induced background with a detailed detector simulation at a 3 TeV collider. The reconstruction algorithms of the physics objects were revised and fine-tuned to preserve their reconstruction efficiency and the accuracy in the determination of their properties.

Moreover, such physics objects were used to carry out sensitivity studies on the Higgs boson production cross sections at a 3 TeV collider. Although preliminary, the results are comparable to the corresponding full-fledged estimates from the CLIC Collaboration at the same collision energy.

### 1.2.4 Work planned for Evaluation Report

The work plan for the Evaluation Report follows two main directions: the completion of the physics objects studies at the 3 TeV center-of-mass energy and a preliminary evaluation of the reconstruction performance for the main physics objects at a 10 TeV collider.

At 3 TeV, the tau leptons are still missing to complete the set of available physics objects. Their reconstruction algorithms must be studied. In addition, only preliminary studies were conducted on the missing energy measurement. As soon as a detector model is available for a 10 TeV muon collider, a preliminary evaluation of the main physics objects reconstruction performance will be carried out.



### 1.2.5 Important missing effort

Some efforts are still missing to get a complete picture of the detector performance at 3 TeV and to have a full set of reconstructed objects to be used in physics studies:

- a study of the reconstruction algorithms for tau leptons with the beam-induced background and an assessment of their performance;
- a refinement of the electron and photon reconstruction: the energy resolution is currently limited at low energies by the high thresholds set for the electromagnetic calorimeter hits and at high energies by the spillage of the electromagnetic showers into the hadronic calorimeter; electron reconstruction would also benefit from the recovery of the radiated bremsstrahlung photons;
- an optimization of the jet reconstruction, taking advantage of an improved reconstruction of low-momentum objects;
- an improvement of the jet flavour identification, exploiting more sophisticated algorithms based on artificial-intelligence techniques.

The same studies have to be then carried out at the center-of-mass energy of 10 TeV.

## 1.3 Technologies (N. Bartosik)

### 1.3.1 System overview

The detector concept described earlier serves as a starting point for evaluating the expected detector performance in different physics scenarios by building an efficient full-simulation workflow to study various BIB-mitigation strategies. At this conceptual stage only general assumptions about the relevant detector parameters were made, such as dimensions, material composition, granularity, spatial and time resolution. This approach simplifies the process of iterative variations towards an optimised detector design for which specific technology details can be implemented at a later stage. These studies allowed to identify the key features of different subdetectors at a Muon Collider experiment, which are summarised in the recent review for Snowmass 2021 on the promising detector technologies and R&D directions [8].

From the technology perspective the present  $\sqrt{s} = 3$  TeV detector model can be divided into six sections ordered by increasing distance from the interaction point:

1. **vertex detector (VXD):** *Si* sensors with  $25 \times 25 \mu\text{m}^2$  pixels and extreme time resolution of  $\sigma_t = 30$  ps arranged in double layers with 2 mm spacing;
2. **inner (IT) and outer (OT) tracker:** *Si* sensors with  $50 \mu\text{m} \times 1$  mm (IT) and  $50 \mu\text{m} \times 10$  mm (OT) macro-pixels and time resolution of  $\sigma_t = 60$  ps;
3. **electromagnetic calorimeter (ECAL):** sampling design with *W* absorber and *Si* sensors arranged in  $5 \times 5 \text{mm}^2$  tiles;
4. **hadronic calorimeter (HCAL):** sampling design with *Fe* absorber and plastic-scintillator tiles arranged in  $30 \times 30 \text{mm}^2$  cells;
5. **superconducting solenoid:** magnetic field strength of 3.57 T with a *Fe* return yoke;
6. **muon detector:** Resistive Plate Chambers (RPC) divided into  $30 \times 30 \text{mm}^2$  cells interleaved in the magnet's return yoke.

Description of this geometry is implemented in the DD4hep [?] framework, which provides interface to Geant4 [3] simulation software and to Marlin [?] framework for detector digitization and event reconstruction. Two generic types of hits are used in the detector simulation:

- **tracker hit:** corresponds to a single energy deposited by a particle in the sensitive volume, with associated energy, time and position of the deposit within the volume;
- **calorimeter hit:** corresponds to the integrated energy deposited by one or more particles in the sensitive volume during the fixed integration time, with only the total energy and time assigned to the hit associated with the volume.

Tracker-type hits are used for VXD, IT and OT detectors, while calorimeter-type hits are used for the ECAL, HCAL and muon detectors, which have the actual granularity implemented in the geometry.

### 1.3.2 Key challenges

High-intensity BIB that survives after passing through the MDI nozzles poses significant challenges for most of the subdetectors by inducing high levels of radiation and by creating excessive amount of background hits. Projected levels of TID and neutron fluence at Muon Collider are comparable to those expected at HL-LHC, while the background hits have signatures unique to Muon Collider and require dedicated treatment in each subdetector to achieve the necessary physics performance.

In the tracking detectors BIB causes very high hit density, up to  $5 \times 10^3$  hits/cm<sup>2</sup> in the innermost layers of VXD, when integrating over a 15 ns readout window. Combinatorial background arising from such a large number of hits makes track reconstruction unfeasible unless the amount of background hits entering the pattern recognition algorithm is significantly reduced. The primary BIB suppression methods in the tracking detectors are:

1. **timing:** rejection of hits outside of a very narrow time window of about 100 ns (exploiting the characteristic time distribution of BIB hits, as shown in Fig. 1.8);
2. **direction:** rejection of hits inconsistent with pointing at the interaction region by estimating their direction from a stub of two hits in a double-layer;
3. **cluster shape:** rejection of BIB hits represented by wider clusters of pixels due crossing the sensors at a shallower angle;
4. **goodness of fit:** rejection of fake track candidates due to bad  $\chi^2$ .

Considering these aspects, the great challenge for a tracking-detector technology is to provide extreme time resolution and on-detector hit filtering while maintaining low material budget and high radiation tolerance. Low material budget indirectly requires low power density of the readout electronics such that it can be cooled without introducing additional heat-exchanging materials.

In the ECAL and HCAL subdetectors BIB contribution comes primarily from low-energy photons and neutrons respectively, which have a relatively uniform angular distribution across the detector volume. Yet their distribution in time and depth is different from the shower signatures produced by the hard collision, as shown in Fig. 1.9. Given the that the BIB contribution overlaps with that of the signal, it can't be excluded from the readout completely, and has to be subtracted instead at a later stage.

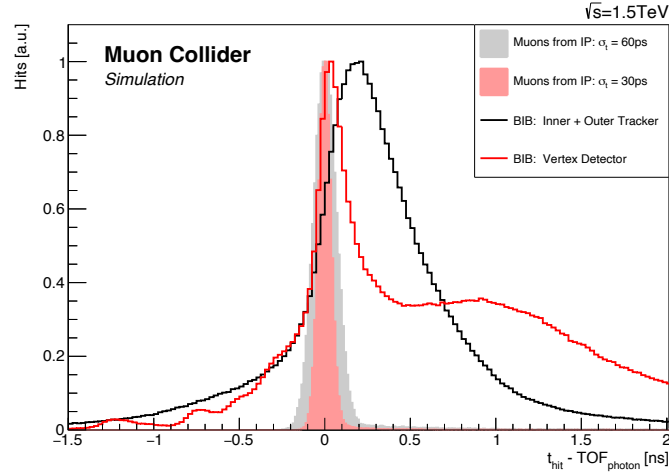


**Fig. 1.8:** Time distribution of hits in the tracking detector corrected for the expected photon's time of flight from the interaction point. Hits from the beam induced background are shown by solid lines, while hits from single muons smeared by corresponding time resolutions are shown by filled areas.

In order to minimise the effect of such BIB subtraction on the resulting energy resolution the corresponding detector should possess high spatial granularity and time resolution, allowing to measure the corresponding time and depth profiles of the shower. In particular fine depth segmentation puts implies a large number of sensitive layers in the detector, making the cost of the technology also an important factor. Thus, the main challenge for the ECAL and HCAL technologies is to provide excellent time resolution in a finely segmented detector at a low cost, while being compatible with the radiation-hardness requirements.

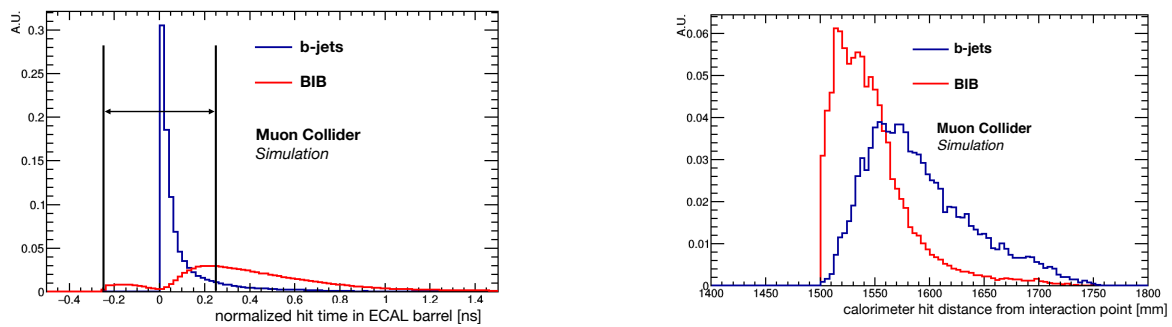


**Fig. 1.9:** Difference between the time (left) and depth (right) of the hits produced by beam-induced background and signal b-jets.

Muon system is relatively unaffected by the BIB contribution except for the very forward region, where high-energy neutrons and photons create hits near the MDI nozzles. While this does not pose any serious challenge for muon detection itself, it is nevertheless important to have high spatial and time resolution to allow matching of standalone muon tracks with hits in the tracking detector. Such seeding of muon tracks from the muon system would greatly improve muon-reconstruction speed given the high combinatorial background in the tracking detector.

### 1.3.3 Work progress since Roadmap

Several developments have been done for different subdetectors towards a better definition of their technical characteristics.

A realistic digitization algorithm for pixel sensors of the tracking detectors has been implemented and intergrated into the Muon Collider simulation software. With a configurable pixel pitch for the sensor together with other readout parameters like noise and threshold it provides realistic pixel clusters that can be used for BIB suppression.

For ECAL a new conceptual design has been implemented in the simulation based on Crilin technology, which is a semi-homogeneous calorimeter with finely segmented Cherenkov-radiating crystals providing high time resolution at relatively low cost. After showing a good performance in simulation studies several physical prototypes have been built and tested to experimentally validate this technology. The latest beam test of a multi-layer prototype at CERN demonstrated a time resolution of  $\mathcal{O}(20\text{ ps})$  and good agreement with Monte Carlo simulations, as shown in Fig. 1.10.

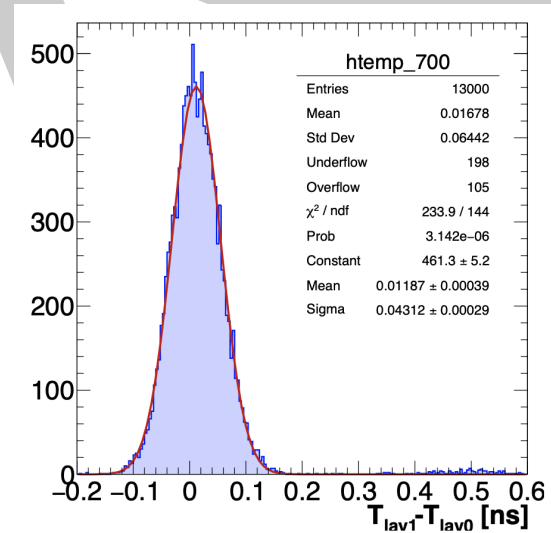
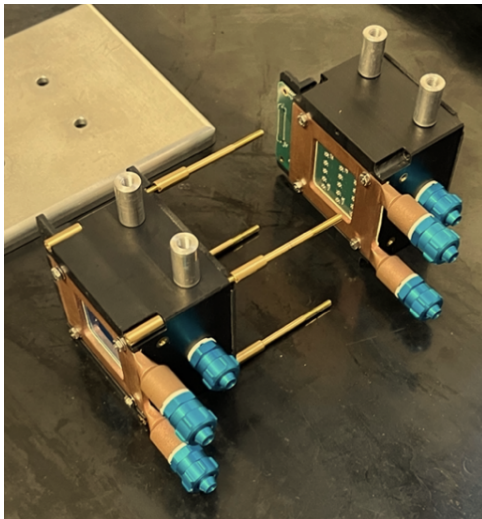


**Fig. 1.10:** Left: two out of three detection layers of the Crilin prototype tested at CERN. Right: Distribution of the time difference between two neighbouring layers of the prototype.

For HCAL the use of Micro-Pattern Gas Detectors (MPGD) as an active layer is under study, which offers good energy and time resolution at high rate and low cost for instrumenting such a large area. The corresponding design has been implemented in the detector geometry for full-simulation studies, which showed performance comparable to that of the current baseline. The technologies being considered are  $\mu$ RWell, RPWell and MicroMegas, for which initial digitization logics for digital readout has been implemented in the simulation software. Physical prototypes for each technology have been also produced and two testbeam campaigns have been carried out at CERN during 2023 (see Fig. 1.11), which showed good results in terms of MIP detection efficiency.

For muon detector the Picosec technology is being studied as a better-performing and cheaper alternative to the RPC active layer. It uses a gaseous Cherenkov radiator coupled to a semi-transparent photocathode via a two-stage amplification by Micromegas, providing time resolution comparable to that of the tracking detector at a relatively low cost. Several prototypes have been tested with different photocathode materials and gas mixtures, with very promising preliminary results, as shown in Fig. 1.12.

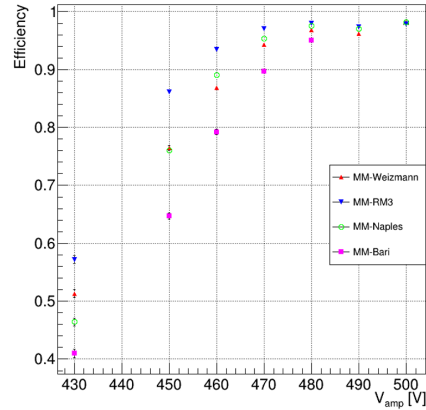
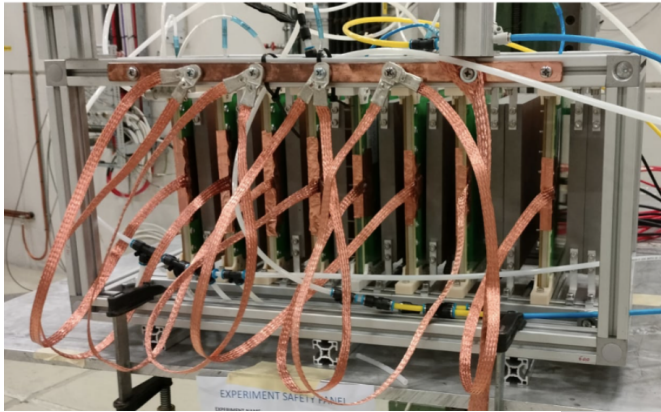


**Fig. 1.11:** Left: MPGD-based HCAL prototype tested at CERN having multiple layers built with different technologies. Right: measured MIP-detection efficiency of different MicroMegas layers as a function of the applied high voltage.

Finally, the tested Picosec geometry has been interfaced with the full-simulation framework to study its performance in the forward region in the presence of BIB.

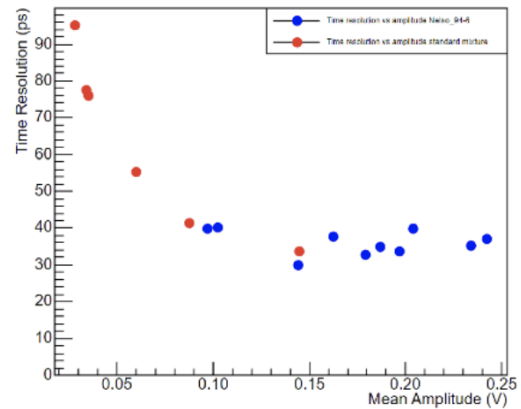
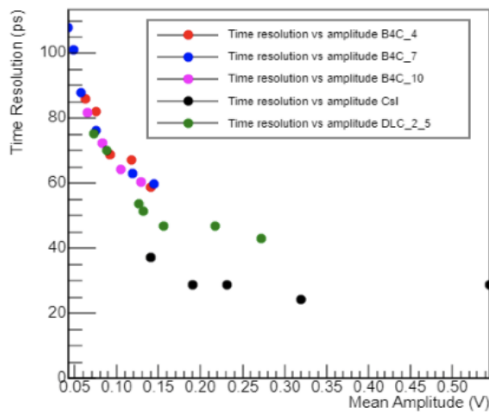


**Fig. 1.12:** Time resolution obtained by the Picosec prototypes as a function of the mean signal amplitude compared for different photo-cathode materials (left) and gas mixtures (right).

To discuss the practical aspects of implementing magnetic field in the Muon Collider detector a dedicated workshop [9] was held at CERN bringing together experts from the detector-simulation and magnet-construction communities. A number of important technological limitations have been outlined as a result, particularly focusing on the material and size requirements posed by strong magnetic fields foreseen at a  $\sqrt{s} = 10$  TeV Muon Collider.

Finally, a number of technical improvements to the full-simulation workflow have been made to significantly reduce the amount of computing resources and time necessary to simulate and reconstruct a complete bunch-crossing event, most of which are described in [10]. The notable optimisations include the early exclusion of irrelevant BIB particles from GEANT4 simulation, filtering and angular splitting of tracker-hit collections, as well as integration of ACTS track-reconstruction framework [11]. Transition to the common Key4hep software stack has also started, which will increase synergies with other future experiments.



### 1.3.4 Work planned for Evaluation Report

A number of developments are planned to progress towards a well-defined conceptual detector design. Important input is expected from experimental tests of the first production batches of DC-RSD sensors, which is a promising technology for the tracking detector. In particular its ability to achieve low occupancy by controlling the extent of charge sharing will be validated and implemented in the simulation software. R&D on the technologies considered for the ECAL, HCAL and muon detector will continue according to their working plans, which are part of the coordinated DRD and CPAD efforts in Europe and U.S. respectively. Finally, a new design of the detector magnet for  $\sqrt{s} = 10$  TeV will be defined, taking into consideration the outcome of the detector-magnet workshop.

### 1.3.5 Important missing effort

All the subdetectors have one candidate technology that is being worked on, which is sufficient to move forward. Yet the lack of alternative new technologies developed in the context of Muon Collider makes it less likely to achieve the best possible physics performance.

This lack of new technologies is particularly important in the tracking detector, where the technology is at a very early stage and multiple technical aspects need to be addressed. These include the possibility of having long pixels in the Inner and Outer Trackers, where hit density is lower, which is challenging to implement in DC-RSD technology. Different possible readout implementations can have great impact on the sensor's efficiency, granularity of the timing information and the resulting power consumption. An integrated approach to the tracker design that also includes the mechanics and cooling will be very important in the future.

## References

- [1] CLIC collaboration, CERN-2012-003
- [2] K.M. Black *et al.*, FERMILAB-FN-1194
- [3] J. Allison *et al.*, *Recent developments in GEANT4*. *Nucl. Instrum. Meth. A* **835**, 186 (2016).
- [4] N. Bartosik *et al.*, *Full Detector Simulation with Unprecedented Background Occupancy at a Muon Collider*, *Comput Softw Big Sci* **5**, 21 (2021).
- [5] M. Frank *et al.*, *DD4hep: A Detector Description Toolkit for High Energy Physics Experiments*, 2014 *J. Phys.: Conf. Ser.* **513** 022010.
- [6] F. Gaede, *Marlin and LCCD—Software tools for the ILC*, *Nucl. Inst. Meth. A* **559**, 177 (2006).
- [7] M. Thomson, *Particle flow calorimetry and the PandoraPFA algorithm*, *Nucl. Inst. Meth. A* **611**, 25 (2009).
- [8] S. Jindariani *et al.*, *Promising Technologies and R&D Directions for the Future Muon Collider Detectors* (2022), [arXiv:2203.07224](https://arxiv.org/abs/2203.07224)
- [9] Detector magnet for 10 TeV MuC (CERN, 2023) [Workshop Indico](#)
- [10] N. Bartosik, P. Andreetto, L. Buonincontri, *et al.*, *Full Detector Simulation with Unprecedented Background Occupancy at a Muon Collider*, *Comput Softw Big Sci* **5**, 21 (2021) [doi:10.1007/s41781-021-00067-x](https://doi.org/10.1007/s41781-021-00067-x)



- [11] X. Ai, C. Allaire, N. Calace *et al.*, A Common Tracking Software Project (2021)  
[arXiv:2106.13593](https://arxiv.org/abs/2106.13593)